


RESEARCH ARTICLE

Metabolism study and toxicological determination of mephtetramine in biological samples by liquid chromatography coupled with high-resolution mass spectrometry

Sara Odoardi¹ | Serena Mestria¹ | Giulia Biosa¹ | Raffaella Arfè² |
Micaela Tirri² | Matteo Marti^{2,3} | Sabina Strano Rossi^{1,3} 

¹Department of Healthcare Surveillance and Bioethics, Forensic Toxicology Laboratory, Università Cattolica del Sacro Cuore F. Policlinico Gemelli IRCCS, Rome, Italy

²Department of Translational Medicine, Section of Legal Medicine and LTTA Centre, University of Ferrara, Ferrara, Italy

³Collaborative Center for the Italian National Early Warning System, Department of Anti-Drug Policies, Presidency of the Council of Ministers, Rome, Italy

Correspondence

Sabina Strano Rossi, Department of Healthcare Surveillance and Bioethics, Forensic Toxicology Laboratory, Università Cattolica del Sacro Cuore F. Policlinico Gemelli IRCCS, Rome, Italy.
Email: sabina.stranorossi@unicatt.it

Funding information

Università Cattolica del Sacro Cuore, Grant/Award Number: D1 2020; University of Ferrara, Grant/Award Numbers: FAR 2019, FAR 2020; Anti-Drug Policies Department, Presidency of the Council of Ministers, Italy

Abstract

The emerging market of new psychoactive substances (NPS) is a global-scale phenomenon, and their identification in biological samples is challenging because of the lack of information about their metabolism and pharmacokinetic. In this study, we performed *in silico* metabolic pathway prediction and *in vivo* metabolism experiments, in order to identify the main metabolites of mephtetramine (MTTA), an NPS found in seizures since 2013. MetaSite™ software was used for *in silico* metabolism predictions and subsequently the presence of metabolites in the blood, urine, and hair of mice after MTTA administration was verified. The biological samples were analyzed by liquid chromatography coupled with high-resolution mass spectrometry (LC–HRMS) using a benchtop Orbitrap instrument. This confirmed the concordance between software prediction and experimental results in biological samples. The metabolites were identified by their accurate masses and fragmentation patterns. LC–HRMS analysis identified the dehydrogenated and demethylated-dehydrogenated metabolites, together with unmodified MTTA in the blood samples. Besides unmodified MTTA, 10 main metabolites were detected in urine. In hair samples, only demethyl MTTA was detected along with MTTA. The combination of MetaSite™ prediction and *in vivo* experiment was a powerful tool for studying MTTA metabolism. This approach enabled the development of the analytical method for the detection of MTTA and its main metabolites in biological samples. The development of analytical methods for the identification of new drugs and their main metabolites is extremely useful for the detection of NPS in biological specimens. Indeed, high throughput methods are precious to uncover the actual extent of use of NPS and their toxicity.

KEYWORDS

LC–HRMS, mephtetramine, metabolism study, new psychoactive substances

This is an open access article under the terms of the Creative Commons Attribution-NonCommercial-NoDerivs License, which permits use and distribution in any medium, provided the original work is properly cited, the use is non-commercial and no modifications or adaptations are made.

© 2021 The Authors. *Drug Testing and Analysis* published by John Wiley & Sons Ltd.

1 | INTRODUCTION

The abuse of new psychoactive substances (NPSs) is a global phenomenon. NPSs' market is extremely dynamic and constantly in change in order to both satisfy customers and to circumvent legal authorities.^{1,2} The identification of NPS in biological specimens is a challenging issue for both forensic and clinical toxicology laboratories.³ In fact, NPS can be extensively metabolized, resulting in low amounts of unmodified drug and the formation of numerous metabolites, especially in urine, which is the bodily specimen routinely analyzed. For this reason, metabolism studies are necessary in order to set up analytical methods targeting main metabolites.

Together with synthetic cannabinoids, the most abused NPS worldwide are stimulants, in particular cathinones.

Mephtramine or MTTA (2-((methylamino)methyl)-3,4-dihydronaphthalen-1(2H)-one) is a stimulant NPS that was first reported to the European Early Warning System in 2013 by the United Kingdom⁴; in the same year, it was detected also in material seized in Italy,⁵ right after the ban of main cathinones by the “analogues criterion” law in these two countries. MTTA structure is similar to cathinones, having a carbonyl group adjacent to a phenyl ring, but it differs from this class by the presence of an additional carbon atom between the carbonyl and amine.

The toxicological and pharmacodynamic properties of MTTA are not yet known. Its structure appears to be similar to molecules with stimulant, antidepressant, or appetite suppressant pharmacological activity.^{6,7}

Metabolic biotransformation data for MTTA are scarce as well. One *in vitro* study was published in which only one metabolite was detected.⁶

In this study, we performed MTTA *in silico* metabolism prediction and *in vivo* metabolism experiments on a murine model. Although some differences between human and animal metabolism can occur, *in vivo* experiments using murine model are frequently performed for the identification of potential biomarkers to establish drug consumption.^{8–10} The combination of *in silico* study with *in vitro* or *in vivo* experiments gave satisfactory results for NPS metabolites identification.^{9–14} The *in silico* prediction of MTTA metabolites was performed using MetaSite™ software. The software predicts CYP450 and FMO3 phase I metabolic reactions. Liquid chromatography coupled with high-resolution mass spectrometry (LC–HRMS) using a benchtop Orbitrap mass spectrometer with full scan mass acquisition, also after *in-source* fragmentation, was used for the detection and elucidation of main MTTA metabolites in blood, urine, and hair of Institute of Cancer Research (ICR) mice after administration of the drug.

2 | MATERIALS AND METHODS

2.1 | Chemicals and reagents

MTTA standard (1 mg/mL) was from LGC, Milan, Italy. For the metabolism study, MTTA was from seized materials, characterized by different

methods⁵ to confirm its chemical identity and purified by high-performance liquid chromatography (HPLC) before animal administration. Amphetamine D5 (1 mg/mL) was purchased from Chebios (Rome, Italy); water, acetonitrile, formic acid, methanol, and β -glucuronidase were purchased from Sigma-Aldrich (Milan, Italy); ammonium formate was from Agilent Technologies (Santa Clara, CA, USA).

Working solutions of MTTA and of the internal standard (IS) amphetamine D5 were prepared at a concentration of 1 μ g/mL. Working solutions were stored at -20°C until use.

2.2 | Metabolism study and samples preparation

Male ICR (CD-1®) mice weighing 30–35 g (Centralized Preclinical Research Laboratory, University of Ferrara, Italy) were group housed (five mice per cage; floor area per animal was 80 cm²; minimum enclosure height was 12 cm), exposed to a 12:12-h light–dark cycle (light period from 6:30 AM to 6:30 PM) at a temperature of 20–22°C and humidity of 45–55% and were provided *ad libitum* access to food (Diet 4RF25 GLP; Mucedola, Settimo Milanese, Milan, Italy) and water. The experimental protocols performed in the present study were in accordance with the U.K. Animals (Scientific Procedures) Act of 1986 and associated guidelines and the new European Communities Council Directive 86/609/EEC. Experimental protocols were approved by the Italian Ministry of Health (license n. 335/2016-PR) and by the Welfare Body of the University of Ferrara. According to the Animal Research: Reporting of *In Vivo* Experiments (ARRIVE) guidelines, all possible efforts were made to minimize the animals' pain and discomfort and to reduce the number of experimental subjects.

MTTA was dissolved in saline (0.9% NaCl; Eurospital, S.p.A, Italy) and administered by intraperitoneal injection (volume of 4 μ L/g), which is widely used in rodents as a route of drugging.¹⁵ The dose of MTTA (10 mg/kg; *i.p.*) was chosen basing on preliminary studies showing the pharmacological activity of that dose of MTTA (data not showed). Therefore, we analyzed samples of urine, blood, and hair from eight mice after the administration of an active dose of MTTA (10 mg/kg).

All specimens were collected and suitably pretreated before the analytical phase.

After the MTTA administration, blood was collected from two sets of four group-housed mice at different times. After a blood sampling before the drug administration (blank samples), both sets of mice underwent three blood sampling: The first specimens were sampled after 20–30 min from MTTA injection; the second sampling took place after 120 min for the first set and after 240 min for the other set of mice; lastly, all mice were subjected to a third collection of blood after 300 min from MTTA administration.

A second group of eight mice was used for urine and hair sampling. Samples of urine and hair were collected once before the administration of MTTA in order to obtain blank samples, allowing to better evaluate the results by minimizing any interference from the matrix.

Urine specimens were collected from mice individually placed inside metabolic cages (Ugo Basile SRL, Gemonio [VA], Italy) with free access to water and food. Urine samples were collected every hour for 6 h following the administration of the MTTA dose, then they were collected after 12, 24, and 30 h.

After all urine samplings, the mice were group housed in the animal facilities for at least 1 month. Mice hair was collected after regrowth to evaluate the drug's accumulation.

2.3 | Urine preparation

The urine samples were analyzed both after enzymatic hydrolysis of glucuronates and without hydrolysis.

One hundred fifty microliters of urine samples diluted 1:1 with 0.1% of formic acid water were hydrolyzed with β -glucuronidase at 40°C for 8 h for the evaluation of possible glucuronidation of phase I metabolites.

Both hydrolyzed and untreated urine samples were subsequently added with amphetamine D5 as IS, diluted with acidified aqueous phase, and 10 μ L were directly injected in the LC–HRMS system.

2.4 | Blood preparation

The blood samples were analyzed following a deproteinization step, where 100 μ L of blood spiked with IS amphetamine D5 were added with 100 μ L of methanol and stirred. After centrifugation at 10,000 g, 10 μ L of the clear supernatant were injected in the LC–HRMS system.

2.5 | Hair preparation

About 30 mg of hair from each mouse was weighed and added to IS amphetamine d5 and left at 40°C overnight under sonication in a small volume of mobile phase A, as described elsewhere.¹⁶ Then 100 μ L of the extract was put in a microvial, and 10 μ L was directly injected into the LC–HRMS system.

2.6 | Validation

LC–HRMS method was validated considering the following parameters: limit of detection (LOD) and of quantification (LOQ), linearity, reproducibility, and accuracy. The LOD and LOQ were assessed by analyzing scalar dilutions of MTTA prepared in blank specimens. The linearity of the method was determined by preparing five points calibration curves, in triplicate, by spiking 100 μ L of blood and urine with MTTA in order to obtain the following concentration: 5, 10, 50, 100, and 200 ng/mL and 0.2, 0.5, 1, 1.5, and 2 ng/mg for hair. Three replicates at low and high concentration levels, 5 and 200 ng/mL for blood and urine and 0.2 and 2 ng/mg for hair, were used for the evaluation of reproducibility and accuracy (bias). Reproducibility was evaluated

as the as the percent coefficient of variation (CV%). The accuracy was expressed as the percent deviation of mean calculated value from the theoretical sample concentration.

2.7 | LC–HRMS equipment and method

2.7.1 | Equipment

The LC–HRMS system was composed of a Thermo ULTIMATE 3000 system equipped with an analytical column Thermo Acclaim RSLC 120 C18 (2.1 \times 100 mm, 2.2- μ m particle size), coupled to a Thermo single-stage Orbitrap (Exactive) MS system, interfaced with a heated electrospray ionization (HESI) source. The whole equipment and the column were from Thermo Fisher Scientific (Milan, Italy).

2.7.2 | LC–HRMS conditions

Mobile phase A was ultrapure water with 5-mM ammonium formate and 0.1% formic acid; mobile phase B was methanol/acetonitrile 1:1 with 0.1% aqueous formic acid. All solvents used were LC–MS grade. The analytical column was maintained at 40°C. The injection volume was 10 μ L, and the flow rate was set at 0.4 mL/min. Mobile phase gradient was as follows: 100% A for 1 min, from 0% to 10% of phase B in 0.1 min, linear gradient to 15% B in 4 min, linear gradient to 50% B in 1.8 min, to 70% B in 1.7, to 80% B in 1.1 min, to 100% in 1 min held for 3.5 min. The chromatographic run time was 14.5 min per analysis.

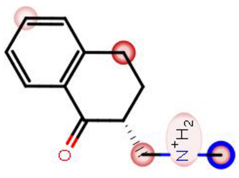
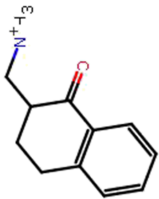
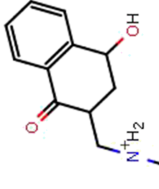
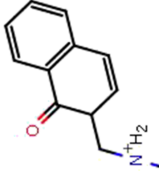
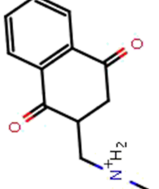
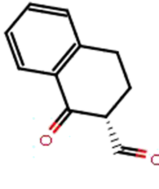
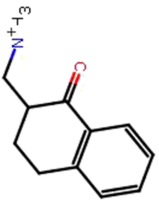
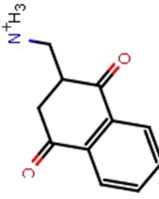
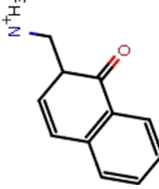
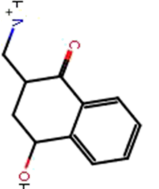
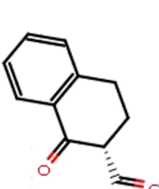
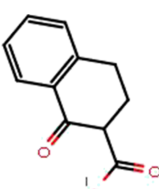
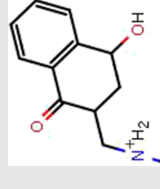
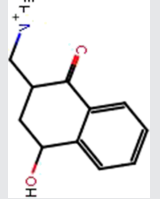
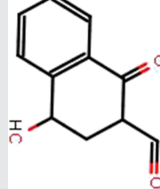
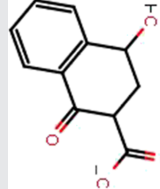
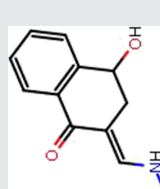
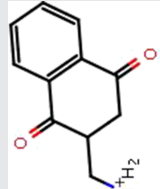
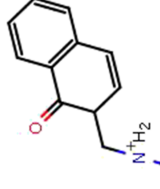
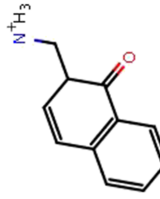
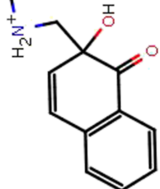
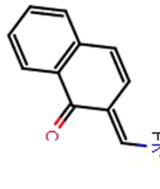
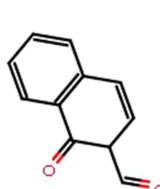
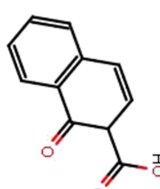
Mass spectrometer was set as follows: Source current was set at 5 μ A, sheath gas and auxiliary gas (either nitrogen) flow rates at 35 and 18 arbitrary units, respectively; capillary temperature at 290°C, the capillary voltage at 45 V, the tube lens voltage at 90 V, the skimmer voltage at 22 V.

Data were acquired in full scan mode over a mass range of 50–750 m/z . The instrument operated in positive ion mode with a resolving power of 100,000 full width at half maximum (FWHM). A further set of experiments was performed with insource collision-induced dissociation (CID) with voltage set at 40 V, acquiring ions from 50 to 750 m/z , with a resolving power of 50,000 FWHM, obtaining the accurate masses of both precursors and fragment ions.

2.7.3 | Modeling metabolism and data analysis

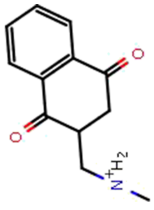
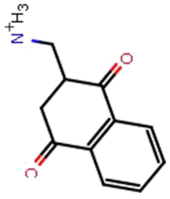
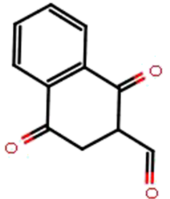
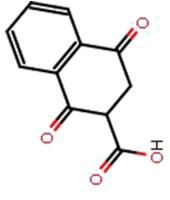
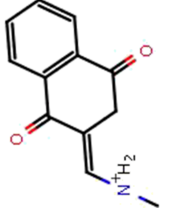
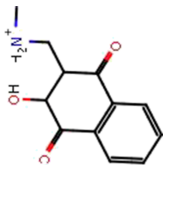
The metabolite prediction was conducted using MetaSite™ software version 3.0 (Molecular Discovery Ltd., UK). The software provided a summary of information about the predicted metabolites, such as their theoretical protonated mass, structures, and molecular formulae. A database with the metabolites predicted, together with other likely metabolites originated from expected metabolic reactions, such as glucuro-conjugation, and their theoretical protonated mass, was created. A manual revision of datafiles was performed in order to search for compounds present in the database. The fragmentation patterns

TABLE 1 MTTA structure, more probable sites of metabolism (SoM), first- and second-generation metabolites predicted by Metasite® software, and their presence in urine (U), blood (B), and hair (H)

First-generation metabolites	
Substrate	Metabolites
 <p>MTTA (U, B, H)</p>	<div style="display: flex; justify-content: space-around;"> <div style="text-align: center;">  <p>Metabolite 1 (U, H)</p> </div> <div style="text-align: center;">  <p>Metabolite 2 (U)</p> </div> <div style="text-align: center;">  <p>Metabolite 3 (U, B)</p> </div> <div style="text-align: center;">  <p>Metabolite 4 (U)</p> </div> <div style="text-align: center;">  <p>Metabolite 5</p> </div> </div>
Second-generation metabolites	
Substrate	Metabolites
 <p>Metabolite 1 (U, H)</p>	<div style="display: flex; justify-content: space-around;"> <div style="text-align: center;">  <p>Metabolite 6 (U)</p> </div> <div style="text-align: center;">  <p>Metabolite 7 (U, B)</p> </div> <div style="text-align: center;">  <p>Metabolite 8</p> </div> <div style="text-align: center;">  <p>Metabolite 5</p> </div> <div style="text-align: center;">  <p>Metabolite 9</p> </div> </div>
 <p>Metabolite 2 (U)</p>	<div style="display: flex; justify-content: space-around;"> <div style="text-align: center;">  <p>Metabolite 8</p> </div> <div style="text-align: center;">  <p>Metabolite 10</p> </div> <div style="text-align: center;">  <p>Metabolite 11</p> </div> <div style="text-align: center;">  <p>Metabolite 12</p> </div> <div style="text-align: center;">  <p>Metabolite 4 (U)</p> </div> </div>
 <p>Metabolite 3 (U, B)</p>	<div style="display: flex; justify-content: space-around;"> <div style="text-align: center;">  <p>Metabolite 7 (U, B)</p> </div> <div style="text-align: center;">  <p>Metabolite 13</p> </div> <div style="text-align: center;">  <p>Metabolite 14 (U)</p> </div> <div style="text-align: center;">  <p>Metabolite 15</p> </div> <div style="text-align: center;">  <p>Metabolite 16</p> </div> </div>

(Continues)

TABLE 1 (Continued)

Second-generation metabolites	Metabolites
Substrate	
	 Metabolite 4 (U)
	 Metabolite 6 (U)
	 Metabolite 17
	 Metabolite 18
	 Metabolite 19 (U)
	 Metabolite 20

of the metabolites were preliminarily predicted using Mass Frontier 1.0 software (Thermo Fisher Scientific) and then manually revised.

3 | RESULTS AND DISCUSSION

MTTA fragmentation pattern was firstly studied. The base peak in the spectrum was m/z 91.0544, related to tropilium ion; other main ions were m/z 147.0805 and m/z 129.0696, corresponding to the tetralone ion and to the ion obtained from the tetralone without a molecule of water, respectively. Other ions detected were at m/z 117.0697 and m/z 105.0701, both with very low intensities.

MTTA molecule was hence used as substrate for Metasite metabolism prediction.

Metasite is able to predict the more probable Sites of Metabolism (SoM) by considering both the reactivity of the positions of the molecule and its interaction with the cytochrome P450 cavity. The software takes into account the 3-D stereoelectronic structure of the enzyme active site and of the substrate and predicts the main metabolites that can be formed in various human tissues (liver, skin, brain, and lungs). Hence, the metabolites predicted are listed with a likelihood ranking. Metabolites generated by the software can be chosen as substrate for further metabolic reactions, giving as result second generation metabolites. On the other hand, Metasite cannot predict phase II metabolites. The software identified the following as the most probable SoM for MTTA: the carbon atom of the methylamino moiety, followed by the carbon in Position 4 of the tetralone moiety and then the carbon in α of the side chain. This is depicted in Table 1, where in MTTA molecule, the most probable site of metabolism is represented by the darkest circle, and the other metabolites gradually with clearer circles. Therefore, Metasite™ predicted the formation of *N*-demethylated, hydroxylated, dehydrogenated, and keto-metabolites as first-generation metabolites. These metabolites can undergo to further metabolic reactions, both of phase I and of phase II (the latter not predicted by Metasite™). Metabolites 1–4, which had more than 50% of likelihood of formation, were chosen as substrate for further metabolic modifications. Table 1 summarizes the main metabolites postulated by the software.

The LC–HRMS analyses performed on authentic samples identified 10 metabolites in the urine of all the mice treated, besides high concentrations of the unchanged drug. The metabolites detected in urine included demethylated MTTA (M1), predicted as the most likely by the software, having 83% of ranking of likelihood, one hydroxylated metabolite (M2), one dehydrogenated (M3), one demethylated and dehydrogenated (M7), two keto-metabolites (M4), one demethylated and carbonylated (M6), one didehydrogenated (M14), and one dehydrogenated and carbonylated metabolite (M19). The hydroxylated metabolite M2 was excreted also as glucuronon-conjugated. The predicted first-generation metabolite 5 (oxidative deamination) was not detected in authentic samples. The identified metabolites, each with its retention time, elemental composition, exact (theoretical) and accurate (measured) mass, mass accuracy as Δ ppm, and fragment ions, are summarized in Table 2. Extracted ion

TABLE 2 Compound, retention time, elemental composition, theoretical protonated exact mass, measured protonated accurate mass, mass accuracy, and principal fragment ions of MTTA and its metabolites

Compound	Retention time (min)	Elemental composition	[M + H] ⁺ Exact mass	[M + H] ⁺ Accurate mass	Mass accuracy (Δppm)	Fragment ions
MTTA	5.1	C ₁₂ H ₁₅ NO	190.1226	190.1222	-2.43	147.0805, 129.0696, 91.0544
Demethyl-MTTA (M1)	5.0	C ₁₁ H ₁₃ NO	176.1070	176.1072	1.47	147.0805, 129.0696, 91.0544
OH-MTTA (M2)	4.7	C ₁₂ H ₁₅ NO ₂	206.1176	206.1178	1.33	163.0766, 103.0550, 107.0499
OH-MTTA glucuronide	1.3	C ₁₈ H ₂₃ NO ₈	382.1496	382.1492	-1.15	/
Dehydro-MTTA (M3)	9.4	C ₁₂ H ₁₃ NO	188.1070	188.1071	0.53	170.0965, 145.0649, 129.0696, 105.0699
Demethyl-dehydro-MTTA (M7)	9.1	C ₁₁ H ₁₁ NO	174.0913	174.0913	0.52	156.0808, 129.0695, 145.0649
Oxo-MTTA metabolite 1 (M4)	8.6	C ₁₂ H ₁₃ NO ₂	204.1019	204.1022	1.25	143.0856, 145.0645, 107.0495
oxo-MTTA metabolite 2 (M4)	8.9	C ₁₂ H ₁₃ NO ₂	204.1019	204.1018	-0.71	143.0857, 145.0645, 107.0495
Demethyl-oxo-MTTA (M6)	7.5	C ₁₁ H ₁₁ NO ₂	190.0863	190.0866	1.70	172.0756, 145.0648, 103.0540
Didehydro-MTTA (M14)	9.2	C ₁₂ H ₁₁ NO	186.0913	186.0918	2.63	168.0811, 157.0649, 158.0965
Dehydro-oxo-MTTA (M19)	8.8	C ₁₂ H ₁₁ NO ₂	202.0863	202.0867	2.10	157.0649, 129.0697

Abbreviation: MTTA, mephtetramine.

chromatograms for MTTA and its metabolites in authentic urine samples are shown in Figure 1. A description of main fragment ions for the each of the main metabolites identified is reported below.

3.1 | Demethyl-MTTA (M1)

The demethyl-MTTA metabolite (2-(aminomethyl)-3,4-dihydro-2H-naphthalen-1-one) showed a retention time close to MTTA (5.0 and 5.1 min, respectively). The fragmented spectra of the two compounds, differing exclusively for the presence of a methyl group, shared some of the main ions, such as m/z 147.0805, relative to the tetralone ion, which was the most abundant ion in the spectrum, m/z 129.0699, the dihydronaphthalene ion, obtained by the loss of a water molecule from the tetralone ion, and the tropilium ion (m/z 91.0541). Fragmented spectrum for demethyl-MTTA is shown in Figure 2. According to Metasite™, this metabolite is the most probable, with 83% of ranking.

3.2 | Hydroxy-MTTA (M2)

The signal of m/z 206.1176 corresponding to the hydroxylated metabolite was detectable in urine specimens with a more intense signal after hydrolysis. It was not possible to identify the position of the OH moiety in the molecule by mass spectrometry analysis, although it could be in one of the tetralone carbon atoms, likely the C in Position 4, as predicted by the software. In fact, by the study of high-resolution fragmented spectrum, the ion m/z 163.0766, related to a molecule with raw formula C₁₀H₁₁O₂, was detected. This ion corresponds to OH-MTTA after the loss of the aminoalkyl moiety. Other fragment ions found were related to the benzylic ring (m/z 103.0550) corresponding to the formula C₈H₇ and to benzylic alcohol ion, m/z 107.0499 with raw formula C₇H₇O. Figure 3 shows the fragmented spectrum for OH-MTTA. The ranking given by the software for the formation of this metabolite was 58% of likelihood.

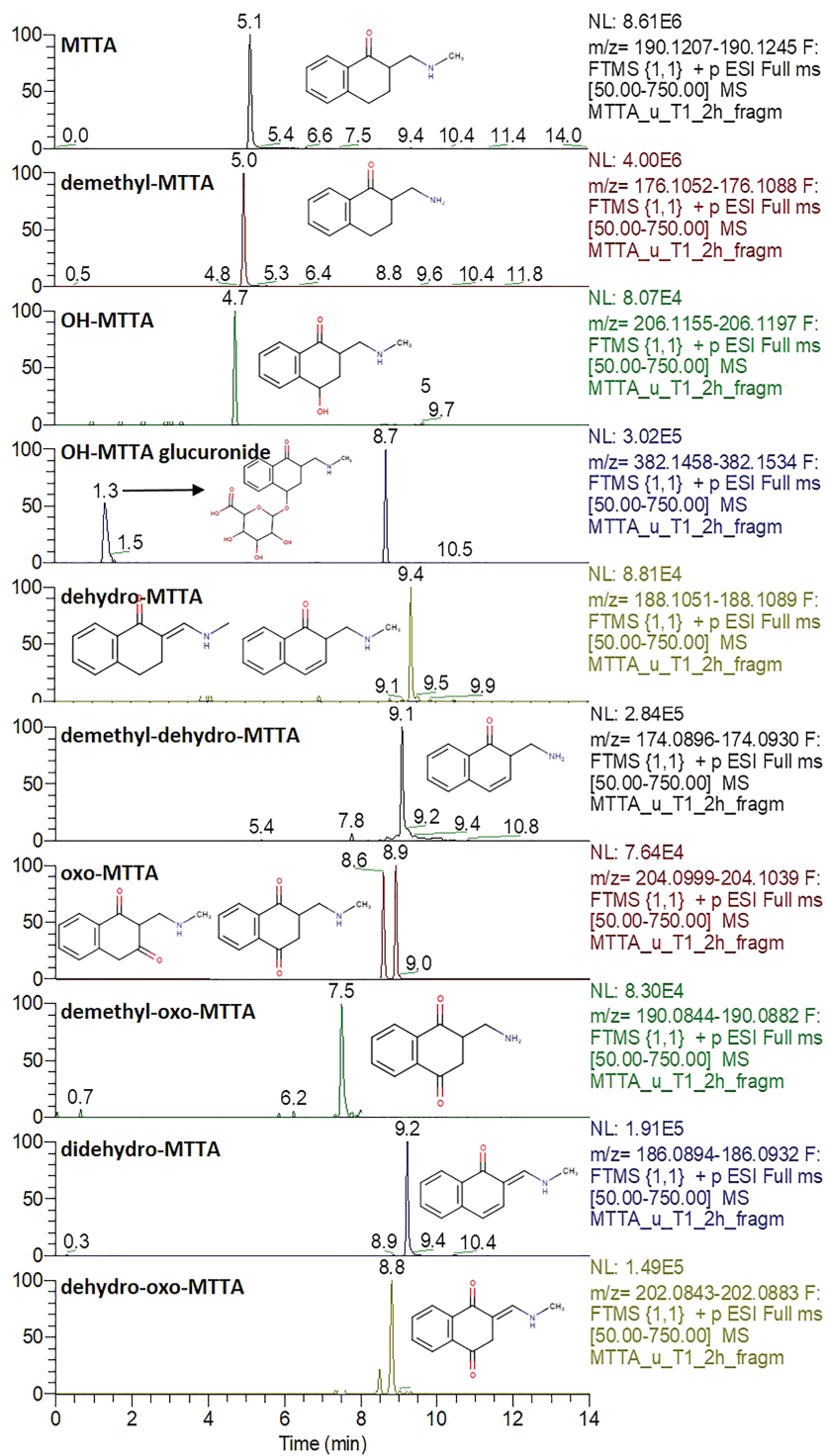


FIGURE 1 Extracted ion chromatograms of the accurate masses of mephtetramine (MTTA) and its postulated metabolites in an authentic urine sample [Colour figure can be viewed at wileyonlinelibrary.com]

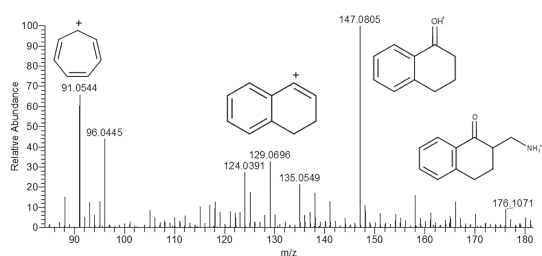


FIGURE 2 Demethyl-mephtetramine (MTTA) (M1) fragmented mass spectrum

3.3 | Dehydro-MTTA (M3)

A dehydro-metabolite (molecular formula $C_{12}H_{13}NO$ and m/z 188.1070) was detected at a retention time 9.4 min. The retention time, higher than the one of MTTA, is compatible with the presence of a less polar molecule, with higher lipophilicity in reversed-phase chromatography, compared with the unmodified drug, such as the dehydro-MTTA, M3. Metasite™ suggested the formation of the dehydrogenated metabolite M3 with a likelihood of formation of 58%.

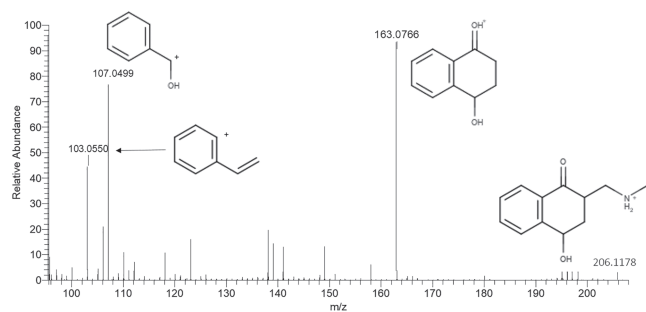


FIGURE 3 OH-mephtetramine (MTTA) (M2) fragmented mass spectrum

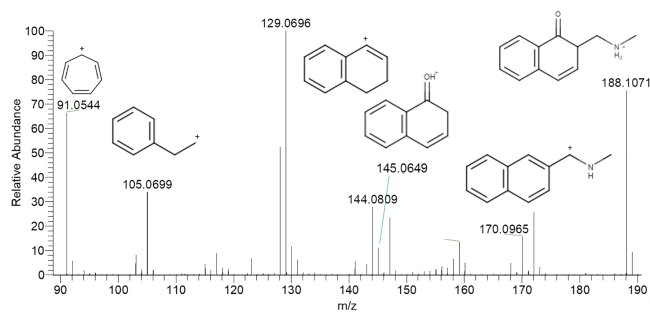


FIGURE 4 Dehydro-mephtetramine (MTTA) (M3) fragmented mass spectrum [Colour figure can be viewed at wileyonlinelibrary.com]

High-resolution fragment ions detected were compatible with this hypothesis, as shown in Figure 4. Fragment ions detected were m/z 170.0965, related to dehydro-MTTA after the loss of a molecule of water, which is a common fragmentation pathway for cathinones,⁵ m/z 145.0649, relative to the dehydrogenated tetralone ion, together with other ions present in MTTA fragmented spectrum, like m/z 129.0696, 105.0699, and 91.0544. Other isobaric compounds were taken in to account for the raw formula $C_{12}H_{13}NO$. Power et al.⁶ postulated the formation of a di-hydro isoxazole derivative, obtained by *N*-oxidation, cyclization, and dehydration. This hypothesis was discarded because of the presence of the fragment ion at m/z 170.0965, not compatible with the structure proposed. Another possible metabolic product is the dehydrogenated MTTA with an exocyclic double bond. This structure was compatible with the ions found in the fragmented spectrum. The formation of this metabolite was not predicted by Metasite™ software, nevertheless it cannot be excluded, also because of the presence in urine samples of metabolite M19, the postulated dehydro-oxo-MTTA, with an exocyclic double bond. Both possible structures are reported in the extracted ion chromatogram of m/z 188.1070 in Figure 1.

3.4 | Oxo-MTTA (M4)

Two keto-metabolites, M4, with retention times 8.6 and 8.9 min, respectively, were detected. The accurate masses observed for these

metabolites, corresponding to the raw formula $C_{12}H_{13}NO_2$, correspond also to three other metabolites predicted by Metasite™ software, named metabolites 12 and 13 (see Table 1), which match to two hydroxylated-dehydrogenated metabolites. The oxo-metabolite had a higher likelihood ranking, according to the software. The fragmented spectra obtained for the two chromatographic peaks were completely superimposable, leading to the hypothesis of two oxo-MTTA having the keto-group in two different positions. Major fragmented species detected were m/z 145.0645, relative to the elemental composition $C_{10}H_9O$, due to the loss of the alkylamino moiety together with a keto-group, and m/z 143.0854, related to the subsequent loss of a hydrogen molecule. Other fragments detected were 107.0495 and 133.0650, relative to raw formulas C_7H_7O and C_9H_9O , respectively. Fragmented spectrum for oxo-MTTA is shown in Figure 5. Metasite postulated the formation of M4 with a score of 58% using MTTA as a substrate and of 35% and 12% as second-generation metabolite, when the substrates were M2 and M3, respectively. This means that its formation could be derived from different metabolic routes.

3.5 | Demethyl-oxo-MTTA (M6)

The second-generation demethyl-oxo metabolite was found at 7.5 min in the extracted ionic chromatogram of m/z 190.0863. Fragment ion originated from the loss of a water molecule, m/z 172.0756, together with ions at m/z 145.0648 and m/z 103.0540, relative to the subsequent loss of the methylamino moiety and to the ethylbenzene ion, respectively, was observed. Metasite™ assigned to M6 a likelihood of formation of 77.5% when generated from M1. It had a 100% likelihood of formation from M4. It could therefore be formed from two different metabolic pathways.

3.6 | Demethyl-dehydro-MTTA (M7)

The second-generation metabolite demethyl-dehydro-MTTA, M7, m/z 174.0913, eluted at 9.1 min. The loss of water led to the fragment at m/z 156.0808, whereas the subsequent loss of the alkylamino moiety gave m/z 129.0695 ion. Fragmented spectrum is shown in Figure 6.

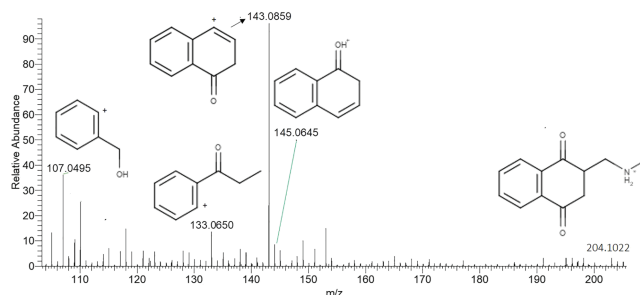


FIGURE 5 Oxo-mephtetramine (MTTA) (M4) fragmented mass spectrum [Colour figure can be viewed at wileyonlinelibrary.com]

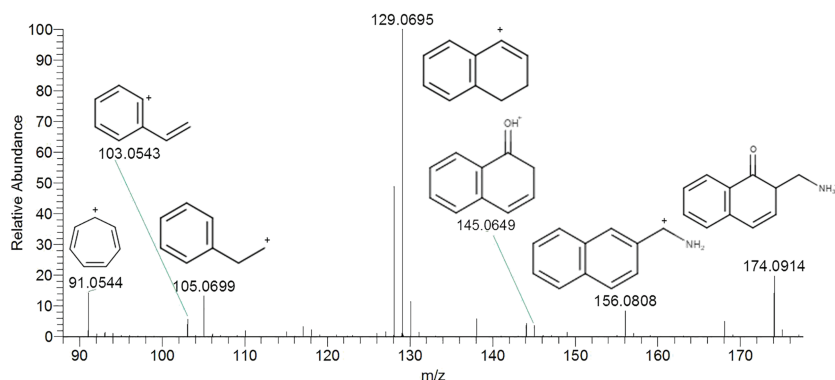


FIGURE 6 Demethyl-dehydro-mephtetramine (MTTA) (M7) fragmented mass spectrum [Colour figure can be viewed at wileyonlinelibrary.com]

M7 Metasite ranking is 77.5% when the substrate is M1, whereas it is 100% using M3 as substrate.

3.7 | Didehydro-MTTA (M14)

A signal in the extracted ion chromatogram relative to the MTTA twice dehydrogenated metabolite, with m/z 186.0913, was detected at 9.2 min. The fragmented spectrum presented the ions at m/z 168.0811, relative to the loss of a molecule of water, the m/z 158.0965, relative to the subsequent loss of the methyl group, and m/z 157.0649, coming from dehydro-MTTA without the methylamino moiety. Metasite™ calculated a score of 45% for M14, using as substrate M3.

3.8 | Dehydro-oxo-MTTA (M19)

Metasite predicts the formation of this second-generation metabolite with a 50% ranking, using M4 as substrate. In the extracted ionic chromatogram of m/z 202.0863, corresponding to its exact mass, a peak was observed at 8.8 min. Fragmented spectrum was quite poor, showing only ions at m/z 157.0649 and m/z 129.0697, compatible with the postulated structure.

After hydrolysis, only the signal related to OH-MTTA increased whereas the peak of the glucuro-conjugated OH-MTTA was no longer present. The areas of the peaks of the other metabolites were not modified; consequently, it is likely that they were excreted only in the free form.

3.9 | Method validation

The validation results obtained for the LC–HRMS method for the detection of MTTA in the different matrices are the following: The LOD was 2 ng/mL for blood and 1 ng/mL for urine, and LOQ was 5 ng/mL for blood and 2 ng/mL for urine; the LOD for hair samples was 0.05 ng/mg and the LOQ 0.2 ng/mg. The linearity range evaluated at 5–200 ng/mL for blood and urine and at 0.2–2 ng/mg for hair showed correlation coefficient of the curves >0.990 for all the

matrices. Reproducibility and accuracy (bias) showed values of %CV and %E not exceeding 15% in both concentrations, acceptable for both the parameters, in the biological matrices studied.

3.10 | Concentration and detection times in biological samples

MTTA concentration in urine specimens, calculated after dilution 1:10 or 1:20 of the samples at higher concentrations, ranged from 1.62 to 7.17 $\mu\text{g/mL}$ in the urine collected after 1 h from the administration, 1.39–6.03 $\mu\text{g/mL}$ after 2 h, 0.93–3.42 $\mu\text{g/mL}$ after 3 h, 288 ng/mL–3.22 $\mu\text{g/mL}$ after 4 h, 92–594 ng/mL after 5 h, 47–326 ng/mL after 6 h, 39–290 ng/mL after 12 h, 8–170 ng/mL at 24 h, and 5–93 ng/mL at 30 h. In absence of analytical standards, no quantification was possible for MTTA metabolites but only an evaluation of the areas of their peaks with respect to the area of the IS. The areas of both MTTA and its metabolites decreased at higher times of urine collection. MTTA, demethyl-MTTA, and OH-MTTA were detectable in all urine samples, meaning at least 30-h postdosing. Dehydro-MTTA, demethyl-dehydro-MTTA, both the oxo-MTTA, demethyl-oxo-MTTA, didehydro-MTTA, and dehydro-oxo-MTTA were detectable only for 4 h after the administration. This suggests that it is of primary importance to include in the screening procedures at least demethyl-MTTA and OH-MTTA. In blood samples, only MTTA, dehydrogenated, and demethylated-dehydrogenated metabolites were detectable. Dehydro-MTTA was detectable only in the 30 min after dosing blood samples while demethyl-dehydro-MTTA up to 180 min after dosing. MTTA concentrations ranged from 7 to 124 ng/mL and was detectable till 180 min after dosing. Surprisingly, no demethylated metabolite was detectable in any of the blood samples, although it was the main urinary metabolite and was present as unique metabolite in hair samples. It could be due to the rapid metabolism in mice,⁸ with the fast transformation of M1 into the second-generation metabolite demethyl-dehydro-MTTA.

MTTA and demethyl-MTTA were detectable in all hair samples analyzed, whereas none of the other metabolites was identified in hair samples. MTTA concentrations in hair ranged from 0.33 to 1.30 ng/mg.

As already reported,^{9–11,13,14} the study demonstrated the good concordance between in silico metabolism prediction and in vivo

results. In fact, among the 20 metabolites predicted by the software, nine were detected in authentic urine samples, and they comprised those with higher likelihood of formation (M1–M4). As expected, not all the predicted metabolites were encountered in mice urine/blood samples. It could be due to differences in mice metabolism respect to human one. Another possible explanation is that other metabolites were formed at concentrations lower than the limit of detection. The study demonstrated the usefulness of the theoretic metabolism prediction, which can be a starting point for developing methods to detect the most likely metabolites, mainly in urine. A further manual revision of the data is anyway advisable.

The excretion study demonstrated that MTTA undergoes extensive metabolism and that the elimination of some of the metabolites is quite fast, disappearing from urine in 5 h after dosing. Demethyl-MTTA and OH-MTTA, rated as the most probable metabolites by Metasite™ software, were on the contrary detected in urine samples till 30-h postdosing, together with unchanged MTTA, whereas MTTA itself was detected for 180 min in blood.

These findings have been used to set up an analytical LC–HRMS method for the identification of MTTA and its main metabolites in biological samples.

This substance has in fact been seized in European Union (EU) territory,^{4,5} and methods able to screen for the main metabolites of NPS, besides the parent compound in biological samples, are necessary for the diagnosis of their use and of intoxications. The development of high-throughput LC–MS-based analytical methods, especially at high resolution, is probably the best option at the moment to perform a wide range screening, especially knowing the characteristics (structure, accurate mass, and characteristic fragments) of the main metabolites to be targeted.¹⁷

4 | CONCLUSIONS

MTTA metabolism study was performed in silico and followed by in vivo experiments. The more likely predicted metabolites were identified in urine and blood specimens from mice, collected at different times after controlled MTTA administration. MTTA underwent to extensive metabolism giving 10 main metabolites in urine. The software Metasite™ was able to predict all the phase I main metabolites detected in vivo. In the authentic urine samples, only one phase II metabolite, OH-MTTA-glucuronide, was also detected. Unchanged MTTA could be detected in all urine samples till 30-h postdosing, besides two main metabolites, demethyl-MTTA and OH-MTTA. In blood samples, dehydro-MTTA and demethyl-dehydro-MTTA were detected, whereas in hair samples, demethyl-MTTA was the only metabolite identified, besides the unchanged MTTA.

The combination of Metasite™ prediction and LC–HRMS analysis of authentic samples from in vivo experiment demonstrated to be a powerful tool for elucidating MTTA metabolism.

This study allowed the development of analytical methods for the detection of MTTA and its main metabolites in biological samples, thanks to the identification of their accurate masses and main fragments.

ACKNOWLEDGEMENTS

This project was supported by the Anti-Drug Policies Department, Presidency of the Council of Ministers, Italy (project: “Effects of NPS: development of a multicentre research for the information enhancement of the Early Warning System”), local funds from the University of Ferrara (FAR 2019 and FAR 2020), and local funds from the Università Cattolica del Sacro Cuore (D1 2020).

ORCID

Sabina Strano Rossi  <https://orcid.org/0000-0001-7530-2968>

REFERENCES

1. United Nations Office on Drugs and Crime. Current NPS Threats - Volume III - October 2020. https://www.unodc.org/documents/scientific/Current_NPS_Threats_Vol.3.pdf, last time accessed 1st February 2021.
2. Grafinger K, Liechti M, Liakoni E. Clinical value of analytical testing in patients presenting with new psychoactive substances intoxication. *Br J Clin Pharmacol*. 2020;86(3):429-436. <https://doi.org/10.1111/bcp.14115>
3. Adamowicz P, Tokarczyk B. Simple and rapid screening procedure for 143 new psychoactive substances by liquid chromatography-tandem mass spectrometry. *Drug Test Anal*. 2016;8(3):652-667. <https://doi.org/10.1002/dta.181>
4. European Monitoring Centre for Drugs and Drug Abuse- Europol, 2013 Annual Report on the implementation of Council Decision 2005/387/JHA. https://www.emcdda.europa.eu/system/files/publications/814/TDAN14001ENN_475519.pdf, last time accessed 1st February 2021.
5. Strano Rossi S, Odoardi S, Gregori A, et al. An analytical approach to the forensic identification of different classes of new psychoactive substances (NPSs) in seized materials. *Rapid Commun Mass Spectrom*. 2014;28(17):1904-1916. <https://doi.org/10.1002/rcm.6969>
6. Power JD, Scott KR, Gardner EA, et al. The syntheses, characterization and in vitro metabolism of nitracaine, methoxypropylamide and mephtramine. *Drug Test Anal*. 2014;6(7-8):668-675. <https://doi.org/10.1002/dta.1616>
7. Bhandari K, Srivastava S, Shankar G, Nath C. Synthesis and appetite suppressant activity of 1-aryloxy-2-substituted aminomethyltetrahydronaphthalenes as conformationally rigid analogues of fluoxetine. *Bioorg Med Chem*. 2006;14(8):2535-2544. <https://doi.org/10.1016/j.bmc.2005.11.032>
8. Fabregat-Safont D, Barneo-Muñoz M, Martínez-García F, et al. Proposal of 5-methoxy-N-methyl-N-isopropyltryptamine consumption biomarkers through identification of in vivo metabolites from mice. *J Chromatogr a*. 2017;1508:95-105. <https://doi.org/10.1016/j.chroma.2017.06.010>
9. Carrola J, Duarte N, Florindo P, et al. Metabolism of N-ethylhexedrone and buphedrone: an in vivo study in mice using HPLC-MS/MS. *J Chromatogr B Anal Technol Biomed Life Sci*. 2020;1159:95-105. <https://doi.org/10.1016/j.jchromb.2020.122340>
10. Mestria S, Odoardi S, Federici S, et al. Metabolism study of N-methyl 2-aminoindane (NM2AI) and determination of metabolites in biological samples by LC–HRMS. *J Anal Toxicol*. 2020;00(00):1-9. <https://doi.org/10.1093/jat/bkaa111>
11. Sandeep L, Ritam R. Metabolic screening in drug development: in-vivo to in-silico. *J Anal Pharm Res*. 2017;6:4-6. <https://doi.org/10.15406/japlr.2017.06.00185>
12. Strano-Rossi S, Anzillotti L, Dragoni S, et al. Metabolism of JWH-015, JWH-098, JWH-251, and JWH-307 in silico and in vitro: a pilot study for the detection of unknown synthetic cannabinoids metabolites. *Anal Bioanal Chem*. 2014;406(15):3621-3636. <https://doi.org/10.1007/s00216-014-7793-9>

13. Swortwood MJ, Carlier J, Ellefsen KN, et al. In vitro, in vivo and in silico metabolic profiling of α -pyrrolidinopentiothiophenone, a novel thiophene stimulant. *Bioanalysis*. 2016;8(1):65-82. <https://doi.org/10.4155/bio.15.237237>
14. Wohlfarth A, Scheidweiler KB, Pang S, et al. Metabolic characterization of AH-7921, a synthetic opioid designer drug: *in vitro* metabolic stability assessment and metabolite identification, evaluation of *in silico* prediction, and *in vivo* confirmation. *Drug Test Anal*. 2016;8(8):779-791. <https://doi.org/10.1002/dta.1856>
15. Marti M, Neri M, Bilel S, et al. MDMA alone affects sensorimotor and prepulse inhibition responses in mice and rats: tips in the debate on potential MDMA unsafety in human activity. *Forensic Toxicol*. 2019;37(1):132-144. <https://doi.org/10.1007/s11419-018-0444-7>
16. Odoardi S, Valentini V, de Giovanni N, et al. High-throughput screening for drugs of abuse and pharmaceutical drugs in hair by liquid-chromatography-high resolution mass spectrometry (LC-HRMS). *Microchem J*. 2017;133:302-310. <https://doi.org/10.1016/j.microc.2017.03.050>
17. Wu AH, Gerona R, Armenian P, et al. Role of liquid chromatography-high-resolution mass spectrometry (LC-HR/MS) in clinical toxicology. *Clin Toxicol (Phila)*. 2012;50(8):733-742. <https://doi.org/10.3109/15563650.2012.713108>

How to cite this article: Odoardi S, Mestria S, Biossa G, et al. Metabolism study and toxicological determination of mephtramine in biological samples by liquid chromatography coupled with high-resolution mass spectrometry. *Drug Test Anal*. 2021;13:1516–1526. <https://doi.org/10.1002/dta.3044>